A97-37158

AIAA-97-3748

Spacecraft Vibration Reduction Using
Pulse-Width Pulse-Frequency Modulated Input Shaper[*]

Gangbing Song   Nick V. Buck[**]   Brij N. Agrawal

Spacecraft Research and Design Center
Department of Aeronautics and Astronautics
U.S. Naval Postgraduate School
Monterey, CA 93943

Abstract

Minimizing vibrations of a flexible spacecraft actuated by on-off thrusters is a challenging task. This paper presents the first study of Pulse-Width Pulse-Frequency (PWPF) modulated thruster control using command input shaping. Input shaping is a technique which uses shaped command to ensure zero residual vibration of a flexible structure. PWPF modulation is a control method which provides pseudo-linear operation for an on-off thruster. The proposed method takes full advantage of the pseudo-linear property of a PWPF modulator and integrates it with a command shaper to minimize the vibration of a flexible spacecraft induced by on-off thruster firing. Compared to other methods, this new approach has numerous advantages: 1) effectiveness in vibration suppression, 2) dependence only on modal frequency and damping, 3) robustness to variations in modal frequency and damping, 4) easy computation and 5) simple implementation. Numerical simulations performed on an eight-mode model of the Flexible Spacecraft Simulator (FSS) in the Spacecraft Research and Design Center (SRDC) at US Naval Postgraduate School (NPS) demonstrate the efficacy and robustness of the method.

1. Introduction

Most modern spacecraft attitude control systems employ several types of actuators including internal momentum exchange devices (e.g., momentum wheels, reaction wheels, control moment gyros) and thrusters. Thrusters must be used in situations when disturbance torques exceed the control authority of momentum exchange devices. Thrusters are capable of much faster reorientation maneuvers. Proportional thrusters, whose fuel valves open proportional to commanded thrust level are complex and often leak fuel. Therefore, proportional thrusters are rarely used in practical space applications. The commonly used thrusters are the constant-amplitude on-off type. On-off thrusters produce discontinuous and nonlinear control actions. These control actions may excite flexible modes of modern spacecraft, which use large, complex, and light weight structures such as solar array panels. Design an on-off thruster control system to provide fine pointing accuracy while avoiding interaction with the flexible structure poses a challenging task.

Research towards this end has been mainly focused into two areas. In one area, efficient methods to convert continuous input commands to on-off signals suitable for controlling on-off thrusters are sought. This problem is often termed thruster control. The other area focuses on modifying an existing command so that it results in less or zero residual vibration of a flexible spacecraft.

The two major approaches for thruster control are bang-bang control (Skaar et al, 1986; Dodds and Williamson, 1984) and pulse modulation. Bang-bang control is simple in formulation, but results in excessive thruster action. Its discontinuous control actions often interact with the flexible mode of the space craft and result in limit cycles. Therefore bang-bang control is not commonly used. On the other hand, pulse modulators are commonly employed due to their advantages of reduced propellant consumption and near-linear duty cycle. In general, pulse modulators produce a pulse command sequence to the thruster valves by adjusting pulse width and/or pulse frequency. Pulse modulators such as psuedorate modulator (Millar and Vigneron, 1976), integral-pulse frequency modulator (Clark and Franklin, 1969; Hablani, 1994), and Pulse-Width and Pulse-Frequency (PWPF) modulator (Bittner, 1982; Wie and Plescia,

---

1984; Anthony et al, 1990) have been proposed. Among these, the PWPF modulator holds several superior advantages such as close to linear operation, high accuracy and adjustable pulse-width and pulse-frequency which provide scope for advanced control. This modulator has been successfully used for thruster control of several spacecraft such as INTELSAT-5, INSAT and ARABSAAT.

Notch filtering and input shaping (Singer and Seering, 1990) are two commonly used methods to modify the input command in order to reduce vibrations of flexible structures. Between these two methods, input shaping has several superior advantages including effectiveness in vibration cancellation, robustness to variations in modal frequency and damping ratio, and suitability for multiple-mode system (Crain et al, 1996). Originally, this method was designed for systems with proportional actuators. Recently, it has been extended to systems with on-off actuators (Pao and Singhose, 1995; Singhose et at, 1996). However, existing approaches require complicated non-linear optimization and often result in bang-bang control action.

In this paper, a new approach integrating an input shaper with a PWPF modulator to provide vibration reduction for a flexible spacecraft is proposed. The control object in this paper is the Flexible Space Simulator (FSS) in the Spacecraft Research and Design Center (SRDC) at U.S. Naval Postgraduate school. The FSS consists of a rigid circular disk representing a spacecraft central body and an attached "L"-shape flexible appendage representing the antenna support structure. To realize this approach on the FSS, a modal analysis is first performed to identify the system modal frequency of the FSS. Next, an in-depth analysis of the PWPF modulator is conducted to recommend parameter settings. Then, a command input shaper is designed and the shaped command is modulated by the PWPF modulator for thruster control. Lastly, robustness analyses are carried out. Numerical simulations performed on an eight-mode model of FSS demonstrate the efficacy and robustness of the method.

2. The Flexible Spacecraft Simulator (FSS)

The Flexible Spacecraft Simulator (FSS) simulates motion about the pitch axis of a spacecraft. As shown in Fig.2.1, it is comprised of a rigid central body and a reflector supported by a "L"-shape flexible appendage. The center body represents the main body of the spacecraft while the flexible appendage represents a flexible antenna support structure. The

flexible appendage is composed of a base beam cantilevered to the main body and a tip beam connected to the base beam at a right angle with a rigid elbow joint. The flexible appendage is supported by one air pad each at the elbow and tip to minimize friction.
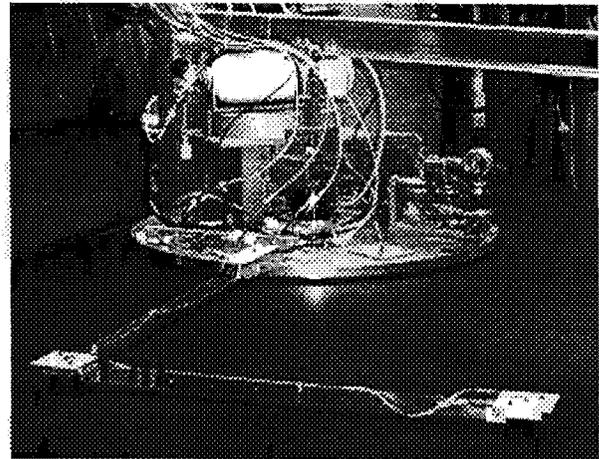

Fig.2.1 The Flexible Spacecraft Simulator (FSS) at U.S. Naval Postgraduate School

The flexible dynamic model used in this study is derived for the FSS (Watkins, 1991 and Hailey, 1992) using the hybrid-coordinate formulation (Likins and Fleischer, 1971). The equations describing the motion of the rigid body and the flexible appendage are

$$I_{zz}\ddot{\theta} + \sum_{i=1}^{n} D_i \ddot{q}_i = T_c + T_d \qquad (2.1)$$

$$\ddot{q}_i + 2\zeta_i \omega_i \dot{q}_i + \omega_i^2 q_i + D_i \ddot{\theta} = T_c + T_d \qquad (2.2)$$

where θ is angular position of the main body, q_i is modal coordinate for the ith cantilever mode, I_{zz} is the moment of inertia of the system, D_i is rigid-elastic coupling for ith mode, T_c is the control torque, T_d is the disturbance torque, ζ_i is the damping ratio of the ith mode, and ω_i is the natural frequency for the ith mode.

The rigid elastic coupling D_i is given by

$$D_i = \int_F \left(x_F \phi_i^y - y_F \phi_i^x \right) dm$$

where x_F and y_F are coordinates of a point on the flexible structure, and ϕ_i^x and ϕ_i^y are respectively the x and y component of ith modal vector at that point.

In discretizing the system via the finite element method, the number of modes was truncated at eight to

obtain a compromise between reasonable model accuracy and computational feasibility. Obtaining sufficiently low cantilever frequency is accomplished by adding point masses at each node as shown in Table 2.1. The base of the "L"-Shaped arm is defined as node zero.

Table 2.1 Nodal Mass Distribution

Node	Point Mass (kg)
1, 2, 3	0.455
4	0.91
5, 6, 7	0.455
8	0.91

The model is placed into state space in preparation for digital simulation using the Matlab/Simulink software package. The state space representation of the system equations is:

$$\dot{x} = Ax + Bu$$

$$y = Cx + Du$$

where the state vector, x, is defined as:

$$x = \begin{bmatrix} \theta & q_1 \cdots q_8 & \dot{\theta} & \dot{q}_1 \cdots \dot{q}_8 \end{bmatrix}^T$$

The output y is the vector of the states, hence C is a 18x18 identity matrix and it is assumed that the feedback values of angular position and rate are measured exactly.

To find the natural frequencies of the flexible-appendage and rigid body system, a Matlab routine is used. The cantilever and system frequencies are listed in Table 2.2. Since low-frequency modes are generally dominant in a flexible system, in this paper, the goal of design is to suppress the low-frequency-mode vibrations

Table 2.2 FSS Cantilever and System Frequencies

Mode	Cantilever		System	
	(Hz)	(rad/sec)	(Hz)	(rad/sec)
1	0.183	1.150	0.213	1.34
2	0.452	2.840	0.504	3.16
3	2.41	15.20	2.42	15.23
4	4.23	26.61	4.25	26.72
5	8.42	52.92	8.42	52.94
6	12.3	77.18	12.3	77.31
7	16.6	104.2	16.6	104.2
8	21.0	132.0	21.0	132.1

3. The PWPF Modulator

The PWPF modulator produces a pulse command sequence to the thruster valves by adjusting the pulse width and pulse frequency. In its linear range, the average torque produced equals the demand torque input. Compared with other methods of modulation, PWPF modulator has several superior advantages such as close to linear operation, high accuracy and adjustable pulse-width and pulse-frequency which provide scope for advanced control.
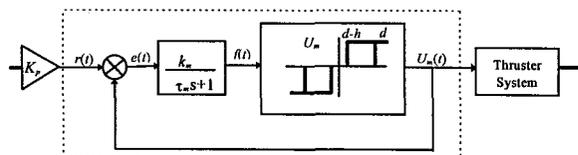

Fig.3.1 The PWPF modulator

As shown in Fig.3.1. the PWPF modulator is comprised of a Schmidt Trigger, a pre-filter, and a feedback loop. A Schmidt Trigger is simply an on-off relay with a deadband and hysteresis. When a positive input to the Schmidt Trigger is greater than d (also denoted as E_{on}), the trigger output is U_m. Consequently, when the input falls below $d-h$ (also denoted as E_{off}), the trigger output is 0. This response is also reflected for negative inputs. The Schmidt Trigger output, U_m, from the feedback loop, and the system input, $r(t)$, form the error signal $e(t)$. The error is fed into the pre-filter whose output $f(t)$ feeds the Schmidt Trigger. The parameters of interest are the pre-filter coefficients k_m and τ_m, input gain K_p, and the Schmidt Trigger parameters d, h, and U_m.

3.1 Modulator Static Characteristics

With a constant input, the modulator has a behavior which is independent of the system in which it is used. The pulse width and period are usually fast compared with the system dynamics so the input to the modulator (the error signal feedback) changes slowly and the static characteristics are a good indication of how the modulator will work in most cases. Choosing appropriate parameters so that the modulator has desired static characteristics is the first step of attitude control design using PWPF modulator.

On-time and off-time

If the input $e(t)$ to the pre-filter is a constant, the relationship between $f(t)$ and $e(t)$ can be represented by

$$f(t) = f(0) + (k_m e - f(0))(1 - e^{-t/\tau_m}) \qquad (3.1)$$

From Eq.(3.1), we have as $t \to \infty$,

$$f(t \to \infty) = k_m e \qquad (3.2)$$

The time taking the pre-filter output to transit from d to d-h is defined as the relay on-time or pulse width, denoted by T_{on} or PW. T_{on} or PW can be solved from Eq.(2.1) by setting $f(0)=d$ and $f(T_{on})=d$-h,

$$T_{on} = PW = -\tau_m \ln\left\{1 + \frac{h}{k_m(r(t) - U_m) - d}\right\} \qquad (3.3)$$

The off time is defined as the time taking the pre-filter output from 0 to d. According to Eq.(3.1), the off time denoted by T_{off} can be solved from Eq.(3.1) by setting $f(0)=0$ and $f(T_{off})=d$,

$$T_{off} = -\tau_m \ln\left\{1 - \frac{h}{k_m r(t) - (d - h)}\right\} \qquad (3.4)$$

Modulator Frequency

The frequency of the PWPF modulator is defined as the inverse of the period of the PWPF cycle and is given by the following equation,

$$f = 1/(T_{on} + T_{off}) \qquad (3.5)$$

i.e.

$$f = \frac{1}{-\tau_m \ln\left[\{1 + \frac{h}{k_m(r - U_m) - d}\}\{1 - \frac{h}{k_m(r - U_m) - (d - h)}\}\right]} \qquad (3.6)$$

Modulation Factor

The modulation factor of the PWPF controller is the ratio of the relay on-time to the period and is given by

$$MF = T_{on}/(T_{on} + T_{off}) \qquad (3.7)$$

i.e.,

$$MF = \frac{1}{1 + \frac{\ln\{1 - \frac{h}{k_m r - (d - h)}\}}{\ln\{1 + \frac{h}{k_m(r - U_m) - d}\}}} \qquad (3.8)$$

Conditions for Pseudo-Linear Operation

The maximum input r_{max} for pseudo-linear operation can be solved by equating the maximum value of the prefilter output $k_m(r_{max} - U_m)$ to the Schimitt Trigger off condition $d - h$,

$$k_m(r_{max} - U_m) = d - h$$

i.e.,

$$(k_m r_{max} - d)/(k_m U_m - h) = 1 \qquad (3.9)$$

or

$$r_{max} = U_m + (d - h)/k_m \qquad (3.10)$$

The effective deadband of the modulator is defined as the minimum input to the modulator so that $T_{on} > 0$. The r_{min} can be determined by equating the prefilter output when the Schimitt Trigger output is zero to the Schimitt Trigger on condition,

$$k_m r_{min} = d$$

i.e.,

$$r_{min} = d / k_m \qquad (3.11)$$

It is clear that increase of k_m reduces the size of deadband. It is reasonable to keep $k_m > 1$ to ensure the on-threshold, d, is an upper bound on the deadband.

With the use of the input gain K_p, the effective deadband is

$$r_{min} = d / (k_m K_p) \qquad (3.12)$$

The net effect of input gain K_p is altering the deadband by scaling the input signal. When an input signal has a large amplitude and does not fall inside the deadband, a small K_p should be used to reduce thruster activity. On the other hand, when the input signal has a small amplitude and falls inside the deadband, a large K_p is required to force the input out of the deadband. In this case, a large K_p can maintain linearity of the modulator and increase control accuracy. Using appropriate K_p according to the magnitude of input signals is an effective way to maintain modulator linearity and reduce thruster activity. In this paper, a two staged input gain K_p will be used as to be discussed in a later section.

Minimum Pulse Width Determination

The effective deadband of the modular is defined as the minimum input to the modulator for which $T_{on} > 0$. Substituting Eq.(3.10) into Eq.(3.4) gives an expression for the minimum on-time, defined as the minimum pulse width. The minimum pulse width is usually dictated by relay operational constrains and is given by

$$T_{min} = -\tau_m \ln\{1 - h/(k_m U_m)\} \qquad (3.13)$$

3.2 PWPF Modulator Design Analysis

The objective of this analysis is to recommend appropriate PWPF modulator parameter settings for general use. The recommended settings will be used

1538

later for design of a PWPF modulator to modulate the command shaped by an input shaper. The design analysis is done by comparing performance indices for different modulator parameter settings with the help of Matlab/Simulink.

3.2.1 Static Analysis

Simulations are performed to study the impact of parameters (E_{on} (d), E_{off} (d-h), k_m and K_p) on the PWPF static performance indices: modulation factor, thruster firing frequency, thruster cycles, and total thruster on-time. To maintain pseudo-linear operation of the PWPF modulator and compromise this objective with total thruster on-time and number of thruster firings, we recommend the preferred range of parameters as listed in Table 3.1. Details of simulations and analysis can be found in Buck (1996).

Table 3.1 Static Analysis Results

Parameter	Recommended Setting
Modulator Gain, k_m	$1 < k_m < 6.0$
On-threshold, E_{on} (d)	>0.3
Off-threshold, E_{off}(d-h)	$< 0.8\, d$
Input Gain, K_p	$2 < K_p < 10$

3.2.2 Dynamic Analysis

To study the impact of input frequency and the time constant on PWPF output phase lag and thruster activity, simulations are conducted by applying unity magnitude sinusoidal inputs to the PWPF modulator. Input frequencies are varied from 1 to 150 rad/sec and time constant are varyied from 0.01 to 0.4. Fixed modulator parameters are shown in Table 3.2 and are consistent with to the recommendations in Table 3.1. The input gain is set to one.

Table 3.2 PWPF Parameters in Dynamic Simulation

Parameter	Simulation Value
K_m	4.5
d	0.45
h	0.15
U_m	1.0

Phase lag

The result of the phase lag simulation is shown in Fig.3.2. The value of phase lag, displayed on the vertical axis, is represented in terms of the percentage of a period of the input signal. For example, zero on the vertical scale indicates no phase lag. A value of 0.5 indicates a phase lag of 50% of a input period.

Note that for τ_m less than 0.2, there is little phase lag for all input frequencies. The plateau shown by a phase lag of 400% indicates the region of zero modulation factor. In this area, the time constant is too large for the modulator to react to the high frequency input. Note that for τ_m greater than approximately 0.2, the phase lag increases monotonically at low frequency. This characteristics is a further reason to maintain τ_m between 0.1 and 0.2 for all applications.
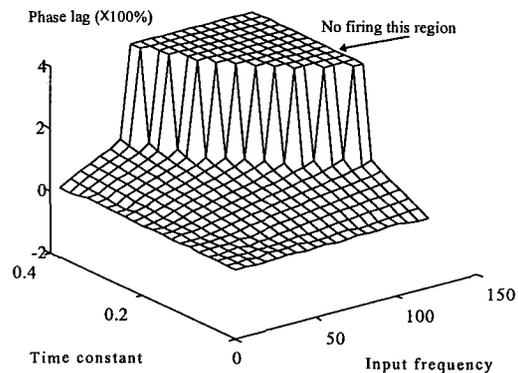

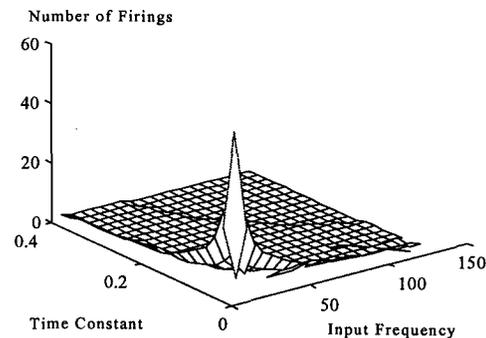Fig.3.2 Phase Lag of PWPF Output
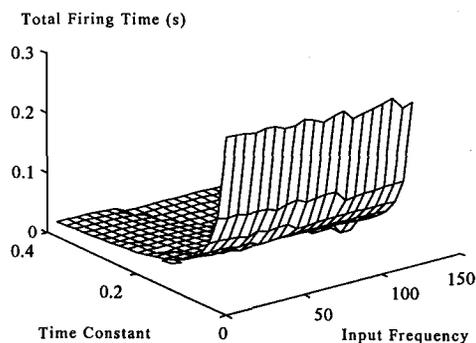

Fig.3.3 Number of Thruster Cycles

Fig.3.4 Thruster On-Time

Thruster activity

Figs.3.3 and 3.4 show the effect of input frequency on thruster activity. Based on the analysis of

thruster activity, a minimum time constant value of 0.1 should be maintained to avoid both frequent thruster firings (Fig.3.3) and excessive propellant use (long thruster on-time) (Fig.3.4).

3.2.3 Fourier Transform Analysis

To better understand PWPF modulation, Fourier transform of the output of a PWPF modulator in pseudo-linear operation is performed and compared with that of the input sinusoidal signal, as shown in Fig.3.5. This figure indicates some minor frequency component in the PWPF output beside the main component (input frequency). These extra frequency components generated by a PWPF modulator must be taken in consideration when it is used to modulate the command of an input shaper.

Fig.3.5 Power Spectral Density Plots

3.2.4 Design Recommendation

The analyses performed in Section 3.2 and 3.3 reveal several consistent trends in PWPF parameter selection. Few of the parameters are worth tuning and the tunable range is relatively small. However, even small modifications in the input gain and the time constant can make a significant difference in achieving the desired performance. Table 3.3 summarizes the results and shows the recommended setting for each parameter.

Table 3.3 Summary of PWPF Design Analyses

	Static Analy.	Dynamic Analy.	Recommended Settings
K_m	$1.0 < 6.0$	N/A	$1.0 < 6.0$
K_p	$2.0 < 10$	N/A	$2.0 < 10$
τ_m	N/A	0.1-0.2	0.1-0.2
d	>0.3	N/A	> 0.3
h	$<0.8d$	N/A	$< 0.8\,d$

Remark 1:

The PWPF parameter settings recommended in Table 3.3 can be used not only in this paper but also as general guidelines for PWPF modulator design.

3.3 Verification of the Recommended Modulator Parameters on FSS Slewing

To verify the PWPF parameter settings in Table 3.4, PWPF modulated thrusters are applied to the FSS to perform a 10-degree slewing. Simulations with input gains (K_p) from 1 to 30 and modulator time constants (τ_m) from 0.02 to 0.9 are performed to study the impact of these two parameters on FSS slewing performance. Values of parameters k_m, d, h, and U_m are given in Table 3.2. The results of the simulations are shown in Figs.3.6-3.8 (rigid-body performance), Figs.3.9-3.10 (thruster activity), and Figs.3.11-3.13 (flexible mode responses).

Time constant, τ_m

As shown in Figs 3.6 - 3.13, the modulator time constant directly impacts the rigid body performance (maximum overshoot and settling time) and flexible modal responses. It is verified that $\tau_m < 0.2$ since in this range the rigid body has less overshoot (Fig.3.6) and less settling time (Fig.3.7) while flexible modes experience less vibration (Figs.3.11 and 3.13). For the lower bound of τ_m, Fig. 3.10 suggests that $\tau_m > 0.1$ so that frequent firing can be avoided while total on-time almost remain at a constant level if $\tau_m < 0.2$ is simultaneously satisfied (Fig.3.9). These results are consistent with Table 3.3.

Pre-filter gain, K_p

The input gain, K_p, is designed to bias the input signal $r(t)$ to keep it outside the deadband. The effective deadband is determined by the product of k_m and K_p, so varying K_p at a fixed value of k_m tailors the deadband without incurring excessive thruster firings. Note in Figs.3.6 - 3.8 show that K_p has little impact on the rigid body performance. This reflects the fact that once K_p is increased to the point where the signal is beyond the deadband, further increases have little effect on the rigid body response. The minimum value of $K_p = 2$ suggested here to guarantee desired performance for most ranges of k_m is also in accordance with the recommended value in Table 3.3.
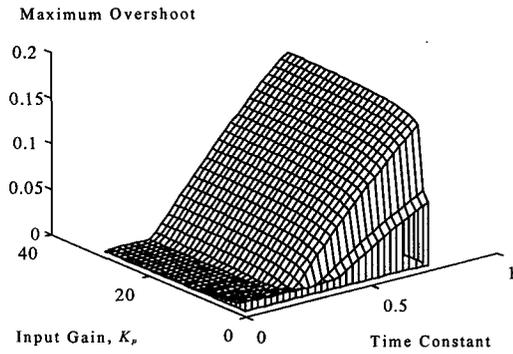
Maximum Overshoot
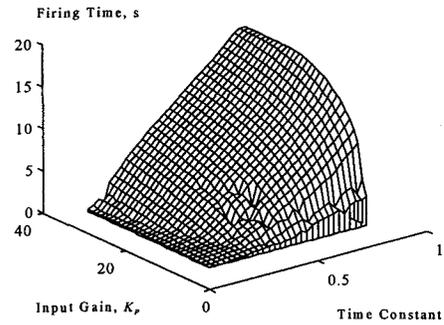
Fig.3.6 Slew Angle Overshoot of Rigid Body

Fig.3.9 Total Thruster On-Time

Fig.3.13 shows that large values of input gain excite specific flexible modes at certain values of the modulator time constant. Figures of higher mode responses (not included here due to space limitation) also confirm this observation. In addition, high input gain values cause an increase in the number (Fig.3.10) and duration of thruster firings (Fig.3.9). To reduce the thruster on-time and number of cycles suggests a ceiling of 10 on K_p. This result is consistent with Table 3.3.
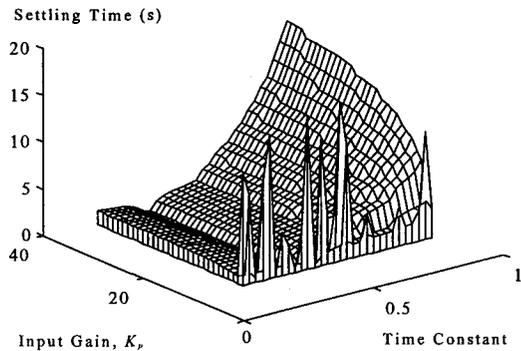
Fig.3.10 Total Thruster Cycles

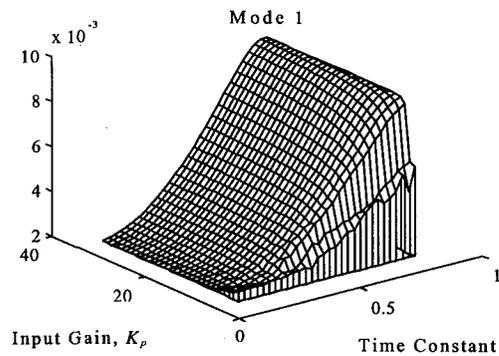Fig.3.7 Rigid Body Settling Time

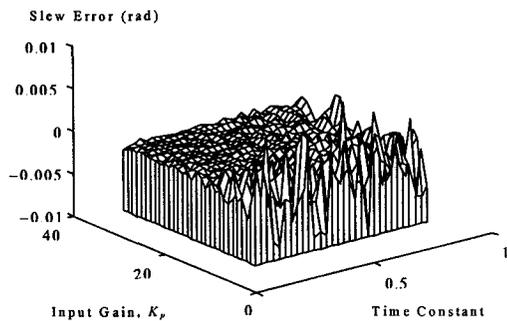Fig.3.11 Response of Mode 1

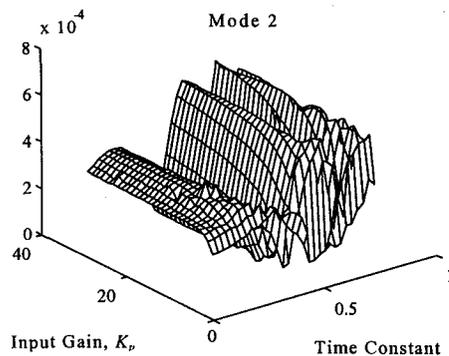Fig.3.8 Final Stage Slew Error of Rigid Body
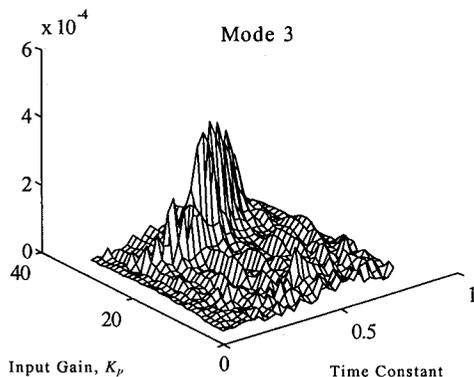
Fig.3.12 Response of Mode 2

1541

Fig.3.13 Response of Mode 3

4. Command Input Shaper

Input shaping is the technique of convolving a sequence of impulses, an input shaper, with a desired command to a flexible structure so that the "shaped command" results in zero residual vibration. This technique is developed based on linear systems theory. A simple illustration of this technique is shown in Fig.4.1. In this figure, the vibration caused by the first impulse can be eliminated by applying an additional impulse of an appropriate amplitude and phase. In this section, some commonly used shapers are reviewed to assist the design of the shaper for the FSS.
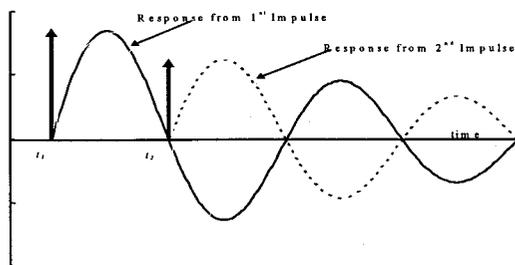

Fig.4.1 Vibration Cancellation using Input Shaping

Consider a linear vibratory system of an arbitrary order, the response of each of its modes to an impulse is given by

$$y(t) = \left[A \frac{\omega_o}{\sqrt{1.0 - \zeta^2}} e^{-\zeta\omega_o(t-t_o)} \right] \sin\left(\omega_0 \sqrt{1.0 - \zeta^2}\, (t - t_o) \right)$$

(4.1)

where A is the amplitude of the impulse, ω_0 is the undamped system natural frequency, ζ is the damping ratio for each of the modes, and t_o is the time of the impulse input. The amplitude of the vibration due to a sequence of impulses is given by

$$A_{amp} = \sqrt{\left(\sum_{j=1}^{N} B_j \cos\phi_j \right)^2 + \left(\sum_{j=1}^{N} B_j \sin\phi_j \right)^2}$$

(4.2)

where

$$\phi_j = \omega\sqrt{(1 - \zeta^2)}\, t_j \quad , \quad B_j = \frac{A_j\omega}{\sqrt{(1 - \zeta^2)}} e^{-\zeta\omega(t_N - t_j)}$$

where A_j is the amplitude of the jth impulse, ω is the system natural frequency, t_N is the time of the final impulse, and t_j is the time of the jth impulse.

Zero Vibration (ZV) Shaper

In order to ensure there is zero vibration at the end of the impulse train, each coefficient B_j in Eq.(4.2) must be identically zero, resulting in two simultaneous "Zero Vibration (ZV)" equations

$$\sum_{j=1}^{N} A_j e^{-\zeta\omega(t_N - t_j)} \sin\left(t_j\omega\sqrt{1 - \zeta^2} \right) = 0$$

$$\sum_{j=1}^{N} A_j e^{-\zeta\omega(t_N - t_j)} \cos\left(t_j\omega\sqrt{1 - \zeta^2} \right) = 0$$

(4.3)

Note that these equations are written in terms of multiple impulses to cancel a single vibrational mode. The shortest pulse train which can cancel a single vibrational mode consists of a two-impulse sequence initiated at $t=0$ with a unity magnitude initial pulse. The amplitude and timing of the second pulse are obtained by solving equations in (4.3) simultaneously. Fig.4.2 shows the resulting impulse train. Note that the impulse train amplitudes have been normalized to unity gain. This procedure is necessary to ensure that the shaper does not scale the original command.
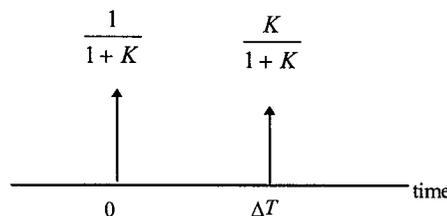

Fig.4.2 Two-Impulse ZV Input

The pulse train parameters are given by

$$K = e^{-\frac{\zeta\pi}{\sqrt{1 - \zeta^2}}} \quad , \quad \Delta T = \frac{\pi}{\omega_o\sqrt{1 - \zeta^2}}$$

(4.4)

Zero Vibration Derivative (ZVD) Shaper

While the ZV shaper provides the shortest impulse

1542

trains, it requires very good knowledge of the plant. Singer and Seering (1990) showed that the ZV shaper was robust for only small variations ($\pm 5\%$) in modal frequency. In order to enhance the shaper's robustness, an additional set of constraint equations can be obtained by differentiating both side of Eq.(4.3) with respect to natural frequency, ω.

$$\sum_{j=1}^{N} A_j t_j e^{-\zeta\omega\left(t_N - t_j\right)} \sin\left(t_j \omega\sqrt{1-\zeta^2}\right) = 0 \qquad (4.5a)$$

$$\sum_{j=1}^{N} A_j t_j e^{-\zeta\omega\left(t_N - t_j\right)} \cos\left(t_j \omega\sqrt{1-\zeta^2}\right) = 0 \qquad (4.5b)$$

Satisfying the additional set of constraints requires two additional variables in the form of an additional impulse (A_3 and t_3). Solving the set of equations yields the impulse train illustrated in Fig.4.3 and quantified by Eq.(4.4). This technique has been shown to provide robustness for up to $\pm 20\%$ variations in frequency (Singer & Seering, 1990).
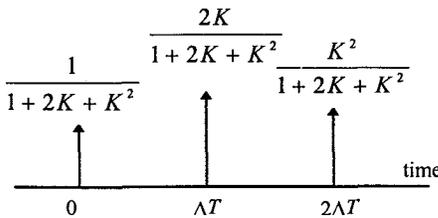

Fig.4.3 Three-Impulse ZVD Input

Zero Vibration Derivative Derivative (ZVDD) Shaper

If the vibration equations are differentiated once again, the resulting vibration will be zero for a range of frequencies above and below the system natural frequency. The effect is to improve robustness dramatically. As noted by various authors, the ZVDD shaper allows plant uncertainties on the order of $\pm 40\%$ while retaining the zero vibration characteristic. The additional constraint equations are obtained by differentiating Eq.(4.5) with respect to ω and setting it to zero:

$$\begin{aligned} \sum_{j=1}^{N} A_j t_j^2 e^{-\zeta\omega\left(t_N - t_j\right)} \sin\left(t_j \omega\sqrt{1-\zeta^2}\right) = 0 \\ \sum_{j=1}^{N} A_j t_j^2 e^{-\zeta\omega\left(t_N - t_j\right)} \cos\left(t_j \omega\sqrt{1-\zeta^2}\right) = 0 \end{aligned} \qquad (4.6)$$

Once again, the additional set of equations requires two more unknowns, A_4 and t_4, so that a total of four impulses are needed in the train to cancel the single vibrational mode. Fig.4.4 illustrates the impulse train for a ZVDD shaper.

Remark 2

With the increase of number of pulses used in the shaper, the shaped command will result in slower rigid body response. Therefore, among ZV, ZVD, and ZVDD shapers, ZV has the fastest rigid body response, and ZVDD has the slowest response.
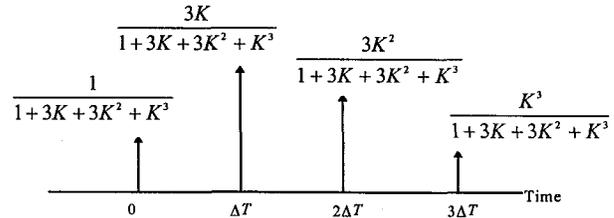

Fig.4.4 Four-Impulse ZVDD Input

Remark 3

For multi-mode flexible systems, the shaper aiming at one fundamental mode may excite a higher mode. But overall performance is still improved.

Constant Amplitude Pulse (CAP) Shaper

ZV, ZVD, and ZVDD shapers are designed for systems with proportional actuators, and they cannot be directly applied to systems with on-off actuators. By imposing constraints of constant-amplitude commands and maneuver requirements ZV, ZVD, and ZVDD shapers are extended to Constant Amplitude Pulse (CAP) Shapers (Pao and Singhose, 1995; Singhose et al, 1996). Obtaining a CAP shaper often involves complicated optimization. CAP shapers also result in bang-bang control action.

Remark 4

Compared with CAP shapers, variable-amplitude shapers like ZV, ZVD, and ZVDD shapers have the advantage of simple computation.

5. Integrated Input Shaper and PWPF Modulator for Vibration Reduction

5.1 The PWPF Modulator

According to the recommended parameter settings in Table 3.3, the parameters of the PWPF modulator are chosen and listed in Table 5.1. This modulator will be used to modulate the command which have been modified by an input shaper.

A two-staged design of K_p is intended to bring the PWPF modulator pre-filter output above the

deadzone leval. When the input falls inside the deadzone a large value is used. Otherwise, the recommended minimum value is used.

Table 5.1 PWPF Parameters

Parameter	Value
K_m	1.25
K_p	2.0, input $> d/k_m$ 5.0, input $\leq d/k_m$
τ_m	0.15
d	0.45
h	0.15

Remark 5

The PWPF modulator parameter settings in Table 3.3 are general recommendations. The PWPF modulator parameters used in this case (shown in Table 5.1) can generally remain the same even when the modulator is used for a different shaper.

5.2 The Input Shaper

As shown in Section 3.3.3, the PWPF modulator does not exactly replicate the input command frequency. This motivates the use of a ZVDD shaper for increased robustness with respect to frequency. Since the goal is to suppress vibrations of low frequency modes, a 4-mode ZVDD shaper is chosen.

Utilizing the design method presented in Section 4, equations (4.3), (4.5), and (4.6) are used to generate the pulse trains for the ZVDD shaper. The resulting four impulse sequence for each mode is given by

$$\text{Mode } i: \quad \begin{bmatrix} A_j \\ t_j \end{bmatrix} = \frac{1}{X_{DD}} \begin{bmatrix} 1 & 3K & 3K^2 & K^3 \\ 0 & \Delta T & 2\Delta T & 3\Delta T \end{bmatrix} \quad (5.4)$$

where K and ΔT are defined in 4.4 and the sequence is unity normalized by

$$X_{DD} = 1 + 3K + 3K^2 + K^3$$

The resulting ZVDD pulse trains for modes 1-4 of the FSS are

$$\text{Mode 1:} \quad \begin{bmatrix} A_j \\ t_j \end{bmatrix} = \begin{bmatrix} 0.1274 & 0.3773 & 0.3726 & 0.1227 \\ 0 & 1.9563 & 3.9127 & 5.8690 \end{bmatrix}$$

$$\text{Mode 2:} \quad \begin{bmatrix} A_j \\ t_j \end{bmatrix} = \begin{bmatrix} 0.1274 & 0.3773 & 0.3726 & 0.1227 \\ 0 & 0.8273 & 1.6547 & 2.8420 \end{bmatrix}$$

$$\text{Mode 3:} \quad \begin{bmatrix} A_j \\ t_j \end{bmatrix} = \begin{bmatrix} 0.1274 & 0.3773 & 0.3726 & 0.1227 \\ 0 & 0.1719 & 0.3437 & 0.5156 \end{bmatrix}$$

$$\text{Mode 4:} \quad \begin{bmatrix} A_j \\ t_j \end{bmatrix} = \begin{bmatrix} 0.1274 & 0.3773 & 0.3726 & 0.1227 \\ 0 & 0.0980 & 0.1960 & 0.2940 \end{bmatrix}$$

Note that the amplitudes are same due to same damping assumed for all modes. The above four impulse trains are convolved to generate the 4-mode ZVDD input as shown in Fig.5.1. For comparison purpose, the unshaped step command is presented in this figure as well. Using the shaped command a longer settling time for the rigid body is expected.
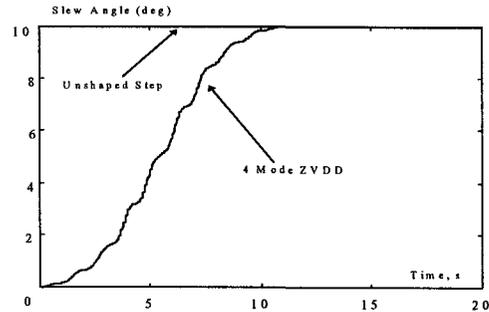

Fig. 5.1 Step and 4-mode ZVDD Commands

5.3 Vibration Reduction Using PWPF Modulated Input Shaper

The PWPF modulator proposed in Section 5.1 is used to modulate the 4-mode ZVDD shaped command proposed in Section 5.2. The primary goal is to reduce lower modes vibration of the FSS during a slewing. As associated with an input shaper, worse performance in higher modes maybe expected, but should be in a limited range. Simulations are done to analyze the impact of the control with PWPF modulated input shaper on rigid body performance and flexible mode responses. The block diagram illustrating the FSS control system is shown in Fig.5.2.
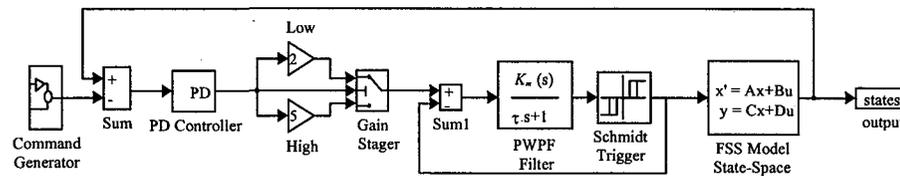
Fig.5.2 The Flexible Spacecraft Simulator with PWPF Modulated Input Shaper

Fig.5.3 shows the lower-mode excitations resulting from a ten-degree slew maneuver. With all modal damping ratios of 0.004, the lower-mode flexible response is essentially undamped for the duration of the simulation when unshaped step command is used. Using a four-mode ZVDD shaper with the PWPF modulator results in excellent cancellation of the targeted modes. Reductions in modal excitations of up to 95% are achieved in the first two modes (Fig.5.3a and 5.3b) and approximately 50% in the third mode (Fig.5.3c). Vibration of mode 4 remain at about the same level (Fig.5.3d).

Increased vibrations are found in modes five and higher (Fig.5.3e - 5.3h). Worse performance in higher modes can be considered as the cost to achieve vibration reduction in lower modes. The increased vibration in higher modes is consistent with other research (Pao and Singhose, 1995). However, in this research, higher modes excitation caused by a shaper designed a lower mode is very limited. Therefore, it can be concluded that vibration reduction using an input shaper and a PWPF modulator is effective for flexible spacecraft with on-off actuators.

Remark 6

If lower modes must be completely eliminated, the multiple-mode shaper (like the 4-mode ZVDD shaper proposed here) does the job at the cost of some excitation of higher-frequency modes. On the other hand, if excitation of higher modes must be avoided and lower-mode vibration should be reduced but not eliminated, a single-mode or two-mode ZVDD shaper can be used.
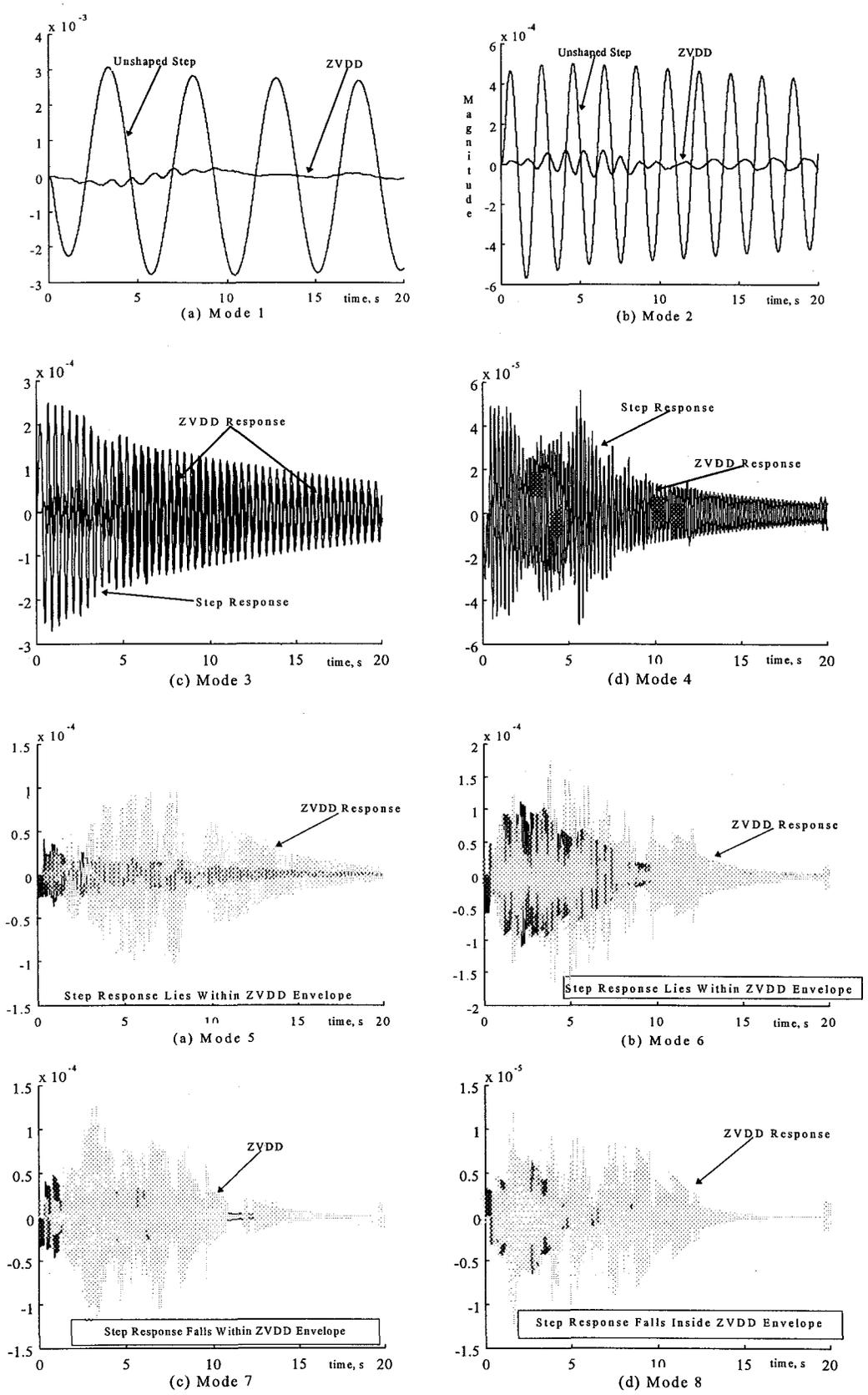
(a) Mode 1

(b) Mode 2

(c) Mode 3

(d) Mode 4

(a) Mode 5

(b) Mode 6

(c) Mode 7

(d) Mode 8

Fig.5.3 FSS Slewing with PWPF Modulated ZVDD Shaper

5.4 Robustness Analysis

Consider that in practice modal frequency can be generally obtained within ±20% error. The first simulation is run with ±20% errors in all 4 modal frequencies of the 4-mode ZVDD shaper and the results are compared with that of the case with exactly known modal frequencies. The rigid body responses are shown in Fig.5.4 and the first two mode responses are shown in Fig.5.5. Fig.5.4 reveals that error in modal frequency slightly changes the settling time, however it has little impact on the final stage error. Fig.5.5a shows the case of -20% frequency error is very close to the nominal case while the case of +20% frequency has a slightly increased vibration. Either case is robust with the error in modal frequency. Fig.5.5b also illustrates that ±20% frequency variations in all four modes have very limited influence on mode 2 vibration. Modes 3 and 4 shows the same trend (figures not shown due to space limitation).
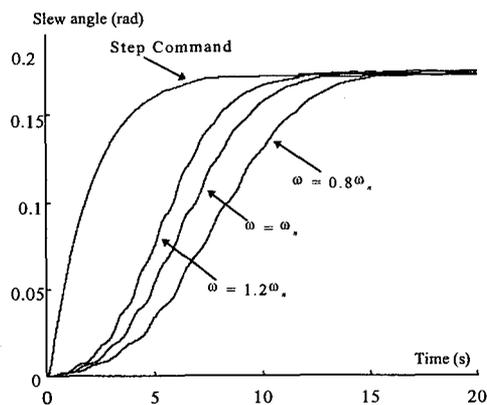

Fig. 5.4 Rigid body response with ±20% modal frequency uncertainty

In order to further study the robustness, simulations are run using frequencies varying from $0.2\omega_n$ to $2.0\omega_n$ and damping ratios varying from 0.1ζ to 2.0ζ for all 4 modes of the 4-mode ZVDD shaper. Flexible mode responses in terms of their average absolute displacement are shown in Figs5.6a - 5.6h. Several observations are made here.

First, vibration increases caused by ±20% modal frequency error are small for the first four modes (Figs5.6a - 5.6d). Modes 6 (Fig.5.6) and 8 (Fig.5.8) are sensitive to under estimated frequency. Since the first four modes are dominant modes and their vibration are well suppressed within ±20% modal frequency error, we conclude that the method is
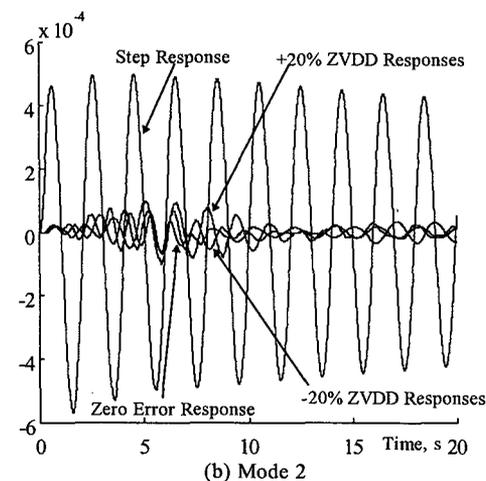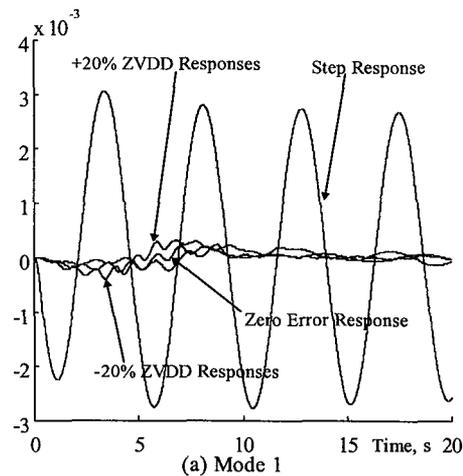
robust to frequency variations.

Fig.5.5 ZVDD shaper robustness to 20% modal frequency uncertainty

Second, Fig 5.6 reveal that the ZVDD shaper is almost insensitive to variations in damping.

Third, use of a PWPF modulated shaper for vibration control achieves well-behaved modal responses even for modal frequency errors of 100%.

The above three observations verify the robustness of the proposed vibration reduction method. In summary, integrating the techniques of command input shaping and PWPF modulation combines the advantages of variable amplitude input shapers and PWPF modulators. It provides a simple, effective, and robust method to suppress vibration on flexible spacecraft.

(a) Mode 1 Average Absolute Displacement

(b) Mode 2 Average Absolute Displacement

(c) Mode 3 Average Absolute Displacement

(d) Mode 4 Average Absolute Displacement

(e) Mode 5 Average Absolute Displacement

(f) Mode 6 Average Absolute Displacement

(g) Mode 7 Average Absolute Displacement

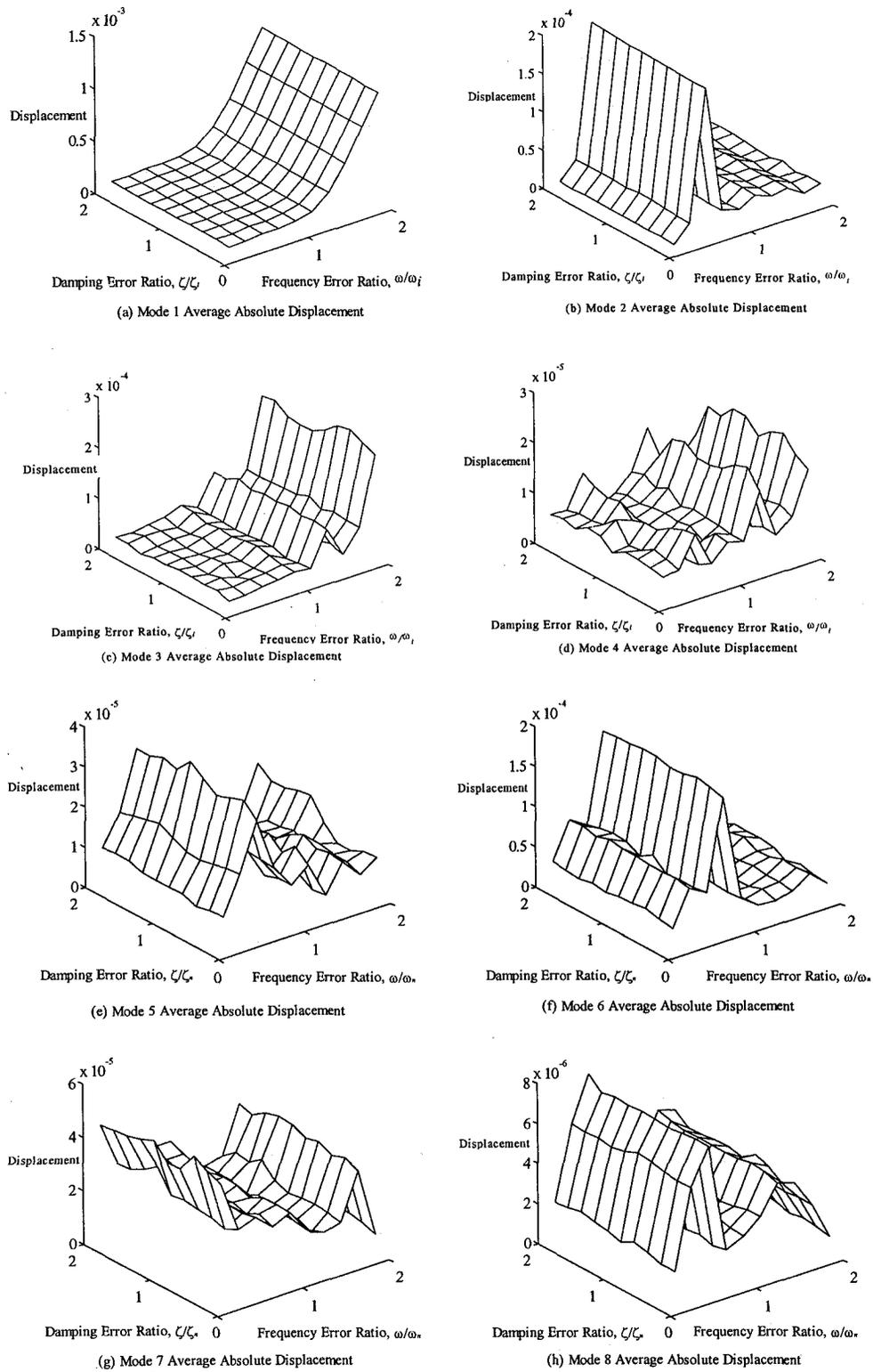
(h) Mode 8 Average Absolute Displacement

Fig.5.6 4-Mode ZVDD Shaper with Modal Frequency Uncertainty and Damping Uncertainty

6. Conclusion

This paper presents the first study of PWPF modulated thruster control using the technique of input shaping. The control object is the Flexible Space Simulator (FSS) at U.S. Naval Postgraduate school. An analytical model of the flexible spacecraft simulator is developed to identify system frequencies. A detailed analysis of the PWPF modulator is performed to study the impact of modulator parameters on its performance. The PWPF modulator analyses reveal a narrow but effective tuning range for some modulator parameters. Subsequent investigations using a two-stage input gain validate the effectiveness of this technique. Use of the recommended design parameter ranges avoids excessive phase lag, minimizes thruster cycles and keeps propellant use to a minimum. A command input shaper is designed and integrated with the PWPF modulator. Robustness analyses are performed to show the insensitivity of PWPF modulated input shapers to frequency and damping uncertainty. Numerical simulations performed on an eight-mode model of the Flexible Spacecraft Simulator (FSS) demonstrate the efficacy of the variable amplitude shaped command with PWPF modulation.

References

Anthony, T., Wei, B., and Carroll, "Pulse-Modulated Control Synthesis for a Flexible Spacecraft," ," AIAA J. of Guidance, Control, and Dynamics, Vol. 13, No. 6, November-December, 1990, pp. 1014-1015.

Bittner, H., Fischer, H.D., and Surauer, M. "Design of Reaction Jet Attitude Control Systems for Flexible Spacecraft," IFAC Automatic Control in Space (Noordwijkerhout, The Netherlands), 1982.

Clark, R.N. and Franklin, G.F., "Limit Cycle Oscillations in Pulse Modulated Systems," J. of Spacecraft and Rockets, Vol. 6, No.7, July 1969, pp. 799-804.

Crain, E., Singhose, W.E, and Seering, W.P, "Derivation and Properties of Convolved and Simultaneous Two-Mode Input Shapers," 13th Triennial IFAC World Congress (San Francisco, CA) 1996.

Buck, N.V., "Minimum Vibration Maneuvers Using Input Shaping and Pulse-Width Pulse-Frequency Modulated Thruster Control," Master Thesis, U.S. Naval Postgraduate School, December, 1996.

Dodds, S.J., and Williamson, S.E., "A Signed Switching Time Bang-bang Attitude Control Law for Fine Pointing of Flexible Spacecraft," International J. of Control, Vol. 40, 1984, pp. 795-811.

Hablani, H.B., "Multiaxis Tracking and Attitude Control of Flexible Spacecraft with Reaction Jets," AIAA J. of Guidance, Control, and Dynamics, Vol. 17, No. 4, July-August, 1994, pp. 831-839.

Hailey, J.A., "Experimental Verification of Attitude Control Techniques for Flexible Spacecraft Slew Maneuvers," Master Thesis, U.S. Naval Postgraduate School, March, 1992.

Likins, P.W. and Fleischer, G.E., "Results of Flexible Spacecraft Attitude Control Studies Utilizing Hybrid Coordinates," J. of Spacecraft and Rockets, Vol.8, March 1971, pp. 264-273.

Millar, A. and Vigneron, F.R., "Attitude Stability of Flexible Spacecraft Which Use Dual Time Constant Feedback Lag Network Pseudorate Control," AIAA/CASI 6th Communications Satellite Systems Conference (Montreal, Canada), April, 1976.

Pao, L. & Singhose, W., "A Comparison of Constant and Variable Amplitude Command Shaping Techniques for Vibration Reduction," 4th IEEE Conference on Control Applications, (Albany, NY), 1995.

Singer, N. & Seering, W., "Preshaping Command Inputs to Reduce System Vibration," Transactions of the ASME, Vol. 112, March 1990.

Singhose, W., Pao, L. & Seering, W., "Time-Optimal Rest-to-Rest Slewing of Multi-Mode Flexible Spacecraft Using ZVD Robustness Constraints," AIAA Guidance, Navigation, and Control Conference, San Diego, CA 1996

Skaar, S.B., Tang, L., and Yalda-Mooshabad, I., "On-Off Control of Flexible Satellites," AIAA J. of Guidance, Control, and Dynamics, Vol. 9, No. 4, July-August, 1986, pp. 507-510.

Watkins Jr., R.J., "The Attitude Control of Flexible Structures," Master Thesis, U.S. Naval Postgraduate School, June, 1991.

Wie, B., and Plescia, C.T., "Attitude Stabilization of Flexible Spacecraft During Stationkeeping Maneuvers," J. of Guidance, Control, and Dynamics, Vol. 7, No. 4, 1984, pp. 430-436.